*Journal of Molecular Structure*, 46 (1978) 395—420



# MORI THREE VARIABLE THEORY AND COMPUTER SIMULATION OF TRANSLATIONAL MOTIONS IN MOLECULAR FLUIDS

A.R. DAVIES, G.J. EVANS and M.W. EVANS
Departments of Applied Mathematics and Chemistry, University College of Wales, Aberystwyth, SY23 1NE, Dyfed, Wales
and G.H. WEGDAM
Physical Chemistry Laboratory, University of Amsterdam, The Netherlands.

## Abstract

The itinerant oscillator model for translational stochastic motion in molecular and atomic fluids is developed using a Mori continued fraction representation of the velocity autocorrelation function $C_v(t)$. The initial generalised Langevin equation is solved in terms of the velocity probability density function and the van Hove self correlation function $G_s(\underline{r},t)$. These are then compared with their equivalents derived independently from molecular dynamics and experimental sources. In particular $C_v(t)$ is compared with velocity a.c.f's computed from an atom-atom intermolecular potential using molecular dynamics methods for four different interatomic separations. The non-Gaussian characteristics of the p.d.f.'s above are investigated using simulations of a.c.f.'s of moments of $\underline{v}$ such as the a.c.f. of kinetic energy. It is concluded that some form of rotation /translation coupling is needed in order that the initial equation may be made more realistic.

## Introduction

The itinerant oscillator model for motion in atomic fluids and uncoupled linear motion in molecular fluids was developed by Sears[1] in 1965 following some speculations by Frenkel[2]. Unfortunately, Sears's paper is mathematically unsound, as was pointed out by Damle et al[3]. In this article we shall use a Mori continued fraction representation[4] of the velocity autocorrelation function, $C_v(t)$, to model the thermal translations of atoms (and molecules) as described by an initial generalised Langevin equation[5]. By use of the Mori continued fraction, itinerant oscillation, i.e. molecular or atomic translations describable by damped oscillations about some equilibrium position which itself diffuses slowly through the bulk fluid can be followed analytically. The initial equations of motion are based on postulates that the random velocity ($\underset{\sim}{v}$) and force ($\underset{\sim}{F}$) in the system are both Gaussian. This is checked directly against molecular dynamics results using the recently developed atom-atom algorithm of Tildesley and Streett[6] to compute $C_v(t)$ and the a.c.f. of force ($\underset{\sim}{F} = m\dot{\underset{\sim}{v}}$), $C_F(t)$; together with those of moments of $\underset{\sim}{v}$ up to the fourth power.

The self part of the van Hove correlation function[7] ($G_s(\underset{\sim}{r},t)$) is evaluated and compared with the experimental neutron scattering results of Dasannacharya and Rao[8(a)] on liquid argon, and the theoretical $C_v(t)$ is compared with the computer simulation of this function for liquid argon carried out by Rahman[8(b)]. This is a good check on internal and interexperimental consistency, since $G_s(\underset{\sim}{r},t)$ can be expressed in terms of $C_v(t)$ using Kubo's second fluctuation-dissipation theorem[9]. By evaluating the speed a.c.f. (that of $|\underset{\sim}{v}|$) and that of the direction of velocity using the atom-atom algorithm, it is shown that a constant speed approximation is valid in treating translational properties of fluids, confirming the results of Berne and Harp[10] for CO.

Theory

We assume that the uncoupled, linear motion of the centre of mass of an atom or molecule of mass in an ensemble of such bodies is governed by the generalised Langevin equation:

$$\dot{\underset{\sim}{v}}(t) + \int_0^t K(t-\tau)\,\underset{\sim}{v}(\tau)\,d\tau = \underset{\sim}{f}(t)/m \qquad (1)$$

where $\underset{\sim}{f}(t)$ is a projected force defined by:

$$K(t) = \langle \underset{\sim}{f}(t)\cdot\underset{\sim}{f}(0)\rangle \frac{m}{3kT}\,. \qquad (2)$$

Since $\langle \underset{\sim}{f}(t)\cdot\underset{\sim}{v}(0)\rangle = 0$ by definition, we have:

$$\dot{C}_v(t) = -\int_0^t K(t-\tau)\,C_v(\tau)\,d\tau, \qquad (3)$$

and further, since K is itself an autocorrelation function (eqn.(2)); it may be shown[10] that:

$$\frac{\partial}{\partial t} K_{n-1}(t) = -\int_0^t K_n(t-\tau)\,K_{n-1}(\tau)\,d\tau \qquad (4)$$

where n = 0,....., N are positive integers. By definition, $K_{-1}(t) \equiv C_v(t)$. No inter-mode coupling (e.g. translation and rotation in molecules), or cross-correlations (describable by $G_d(\underset{\sim}{r},t)$, the distinct part of the van Hove function) are accounted for in eqns. (1) - (4).

The series (4) is a continued fraction in Laplace space (p), so that:

$$\tilde{C}_v(p) = \frac{C_v(0)}{p + \tilde{K}_0(p)} = \frac{C_v(0)}{p + \dfrac{K_0(0)}{p + \tilde{K}_1(p)}} = \cdots\cdots \qquad (5)$$

If now this series is truncated with the assumption that:

$$K_1(t) = K_1(0)\exp(-\gamma t), \tag{6}$$

the resulting expression for $\tilde{C}_v(p)$ is:

$$\tilde{C}_v(p) = \frac{p(p+\gamma) + K_1(0)}{p^3 + p^2\gamma + p(K_0(0)+K_1(0)) + \gamma K_0(0)}. \tag{7}$$

We note that this is <u>formally identical</u> with the solution for $C_v(t)$ of the following equations which are precisely those stochastic differentials[11] needed to describe the physical process of itinerant oscillation[12]:

$$m\ddot{\underset{\sim}{q}}_1(t) + m_1\gamma\dot{\underset{\sim}{q}}_1(t) - m K_0(0)[\underset{\sim}{q} - \underset{\sim}{q}_1] = m_1\dot{\underset{\sim}{w}}_1(t), \tag{8}$$

$$m\ddot{\underset{\sim}{q}}(t) + m K_0(0)(\underset{\sim}{q} - \underset{\sim}{q}_1) = \underset{\sim}{0}, \tag{9}$$

$$K_1(0) = \frac{m}{m_1}K_0(0), \tag{10}$$

$$K_0(0) = \omega_0^2. \tag{11}$$

In this set of equations m is the mass of the atom or molecule whose coordinate is $\underset{\sim}{q}$ and which is surrounded by a diffusing 'cage' of such particles whose centre of mass is at $\underset{\sim}{q}_1$ and whose total mass is $m_1$. The inner particle m is harmonically bound at a frequency $\omega_0$ to the

diffusing cage with a restoring force constant $K_0(o)$. We note that $\underset{\sim}{v} = \dot{\underset{\sim}{q}}$. There is a retarding, frictional force $\gamma \dot{\underset{\sim}{q}}_1$, acting on the diffusing cage due to its surroundings, and $\dot{\underset{\sim}{W}}_1(t)$, which is represented by a statistical Wiener process[12(c)], is the force on the cage caused by random collisions of the Brownian type. Eqns. (8) - (11) give a physical meaning to the abstract truncation represented by eqn. (6).

From the inverse transform of eqn. (7):

$$C_v(t) = \langle \underset{\sim}{v}(t) \cdot \underset{\sim}{v}(o) \rangle / \langle \underset{\sim}{v}(o) \cdot \underset{\sim}{v}(o) \rangle$$
$$= \frac{1}{1+\Gamma}\left[\left(\cos\beta t + \left(\frac{\alpha_1 + \Gamma\alpha_2}{\beta}\right)\sin\beta t\right)e^{-\alpha_1 t} + \Gamma e^{-\alpha_2 t}\right] \quad (12)$$

where

$$\Gamma = \frac{-2\alpha_1\left(\alpha_1^2 + \beta^2\right)}{\alpha_2\left(3\alpha_1^2 - \alpha_2^2 - \beta^2\right)}$$

and $-\alpha_1 \pm i\beta$ ; $-\alpha_2$ are the roots of the secular determinant of eqns. (8) and (9), i.e. the denominator of eqn. (7), for a negative discriminant. For a positive discriminant, $C_v(t)$ is a sum of three real exponentials. These roots may be related to $K_0(o)$, $K_1(o)$, and $\gamma$ by Cardan's formula.

## The $G_s(\underset{\sim}{r},t)$ Function

The self van Hove correlation function may be evaluated by considering eqn. (1) in the form:

$$\ddot{\underset{\sim}{r}}(t) + \int_0^t K(t-\tau)\dot{\underset{\sim}{r}}(\tau)\,d\tau = \underset{\sim}{f}(t)/m \quad (13)$$

where $\dot{\underset{\sim}{r}} = \underset{\sim}{v}$, the velocity of the tagged inner particle of mass m. Now

$G_s(\underset{\sim}{r},t)$ is the probability of finding this particle at $\underset{\sim}{r}$ at time t given that it could be found at $\underset{\sim}{r} = \underset{\sim}{0}$ when t = 0.

In Laplace space, eqn. (13) becomes:

$$\tilde{\underset{\sim}{r}}(p) = \frac{\underset{\sim}{r}(0)}{p} + \frac{\underset{\sim}{v}(0) + \mathcal{L}[\underset{\sim}{f}(t)/m]}{p(p + \tilde{K}(p))} . \tag{14}$$

We have:

$$\mathcal{L}^{-1}\left[p(p+\tilde{K}(p))\right]^{-1} = \int_0^t \frac{\langle \underset{\sim}{v}(t)\cdot\underset{\sim}{v}(0)\rangle}{\langle \underset{\sim}{v}(0)\cdot\underset{\sim}{v}(0)\rangle}\,dt \equiv \Gamma_v(t), \tag{15}$$

so that

$$\begin{aligned}\underset{\sim}{y}(t) &= \underset{\sim}{r}(t) - \underset{\sim}{r}(0) - \Gamma_v(t)\,\underset{\sim}{v}(0) \\ &= \underset{\sim}{r}(t) - \underset{\sim}{r}(0) - \underset{\sim}{r}(t) + \underset{\sim}{r}(0) \\ &= \frac{1}{m}\int_0^t \Gamma_v(t)\,\underset{\sim}{f}(t-\tau)\,d\tau\end{aligned} \tag{16}$$

is the solution of eqn. (13).

Since $\underset{\sim}{f}$ is a Gaussian variate (but non-Markovian)[9,13], the probability distribution of r is a Gaussian also:

$$P(\underset{\sim}{r}(t), \underset{\sim}{r}(0), \underset{\sim}{v}(0); t) = \left[\frac{3}{2\pi B(t)}\right]^{3/2} \exp\left[-\frac{3|\underset{\sim}{y}(t)|^2}{2B(t)}\right]. \tag{17}$$

To obtain $G_s(\underset{\sim}{r},t)$ we must average over all initial $\underset{\sim}{v}(0)$ values, so that:

$$G_s(\underset{\sim}{r},t) = \left[\frac{3}{2\pi B(t)}\right]^{3/2} \exp\left[-\frac{3|\underset{\sim}{r}(t)|^2}{2B(t)}\right]$$

In eqn. (17), $B(t) = \langle \underset{\sim}{y}(t) \cdot \underset{\sim}{y}(t) \rangle$ which we relate to $\Gamma_v(t)$ as follows. Using eqn. (2):

$$B(t) = \frac{3kT}{m} \int_0^t \int_0^t \Gamma_v(t) K(\tau - \tau') \Gamma_v(\tau') \, d\tau \, d\tau',$$

so that:

$$\dot{B}(t) = \frac{6kT}{m} \Gamma_v(t) \mathcal{L}^{-1} \left[ \tilde{K}(p) \tilde{\Gamma}_v(p) \right].$$

Using eqn. (15), and the fact that $\Gamma_v(0) = 0$:

$$\dot{B}(t) = \frac{6kT}{m} \Gamma_v(t) \left[ 1 - \dot{\Gamma}_v(t) \right],$$

$$B(t) = \frac{3kT}{m} \left[ 2 \int_0^t \Gamma_v(t) \, dt - \Gamma_v^2(t) \right]. \qquad (18)$$

Eqn. (18) links $G_s(\underset{\sim}{r},t)$ directly to $C_v(t)$. In classical Brownian motion[14], $C_v(t) = e^{-\beta t}$, so

$$\Gamma_v(t) = \left(1 - e^{-\beta t}\right) / \beta$$

and

$$B(t) = \frac{3kT}{m\beta^2} \left( 2\beta t + 4e^{-\beta t} - e^{-2\beta t} - 3 \right),$$

in agreement with the calculations of Uhlenbeck and Ornstein[15].

In our case the equivalent expressions for B(t) and $\Gamma_v(t)$ are more unwieldy. They are, for itinerant oscillation:

$$\Gamma_v(t) = x_0 \left[ 1 - e^{-\alpha_1 t} \left( \cos \beta t + x_1 \sin \beta t \right) + x_2 \left( 1 - e^{-\alpha_2 t} \right) \right],$$

where

$$x_0 = \frac{2\alpha_1 + \Gamma\alpha_2}{(1+\Gamma)(\alpha_1^2+\beta^2)} ;$$

$$x_1 = \frac{\alpha_1^2 - \beta^2 + \Gamma\alpha_1\alpha_2}{\beta(2\alpha_1 + \Gamma\alpha_2)} ;$$

$$x_2 = \frac{\Gamma(\alpha_1^2+\beta^2)}{\alpha_2(2\alpha_1 + \Gamma\alpha_2)} .$$

So that

$$\int_0^t \Gamma_v(t)\,dt = x_0\left[t - \left(\frac{\alpha_1+x_1\beta}{\alpha_1^2+\beta^2}\right)\left(1 - e^{-\alpha_1 t}\left(\cos\beta t + \left(\frac{\alpha_1 x_1 - \beta}{\alpha_1 + x_1\beta}\right)\sin\beta t\right)\right) + x_2\left(t + \frac{e^{-\alpha_2 t} - 1}{\alpha_2}\right)\right] .$$

However, $G_s(\underset{\sim}{r},t)$ is easily computed given $K_0(o)$, $K_1(o)$ and $\gamma$ obtained from a non-linear least-mean-squares fitting[16] to a simulated $C_v(t)$, or a simulated $C_F(t)$.

Velocity p.d.f.

The solution of eqn. (1) is:

$$\underset{\sim}{v}(t) = \underset{\sim}{v}(t) - C_v(t)\underset{\sim}{v}(o) = \frac{1}{m}\int_0^t C_v(t-\tau)\,\underset{\sim}{f}(\tau)\,d\tau$$

so that it is possible to obtain the probability distribution function of velocities as:

$$P\left(\underset{\sim}{v}(t), \underset{\sim}{v}(0); t\right) = \left[\frac{3}{2\pi A(t)}\right]^{3/2} \exp\left[-\frac{3\left|\underset{\sim}{z}(t)\right|^2}{2A(t)}\right]; \qquad (19)$$

where

$$A(t) = \langle \underset{\sim}{z}(t) \cdot \underset{\sim}{z}(t) \rangle = 3\frac{kT}{m}\left[1 - C_v^2(t)\right].$$

It is possible further to test any non-Gaussian property of $P(\underset{\sim}{v}(t), \underset{\sim}{v}(o); t)$ by molecular dynamics computations[10] of a.c.f.'s of moments of $\underset{\sim}{v}$, such as the kinetic energy a.c.f. This is done below. Eqn. (19) is illustrated in the appendix.

Computation.

The Newton equations for 256 dumbell molecules constrained initially on an $\alpha$-$N_2$ type lattice are solved by the predictor-corrector method with a time-increment of about $5 \times 10^{-15}$ secs. The atom Lennard-Jones parameters $\epsilon/k$ and $\sigma$ are always those for nitrogen, so we have a 'real' molecule only when the interatomic distance d* (in the reduced units of Tildesley and Streett[6]) is 0.3292. The thermodynamic stability of the system is judged on criteria such as the constancy of the total pressure, calculated by the virial theorem[17], and the total internal, or configurational, energy per molecule. Mean square force terms were calculated with 1600 time steps and ensemble (time and number) averaging. The first few hundred time steps are

unstable and are rejected in forming any average. The stability of the computed a.c.f.'s was judged by comparison of runs using 200 and 400 steps. Generally 400 were sufficient since these functions decay rapidly in comparison. Using the two-centre potential builds on an anisotropic repulsion core, while the dispersive part is cut off at about $3.2\sigma$, so that the whole is representative of geometrical and electrostatic anisotropy. The computations were carried out via the Aberystwyth-U.M.R.C.C. CDC 7600 link in approximately 20 minute segments of real time.

## Results

The atom-atom computed force, velocity, speed, and direction of velocity a.c.f.'s are shown, in fig.(1) along with the l.m.s. best fits[16] for the force ($m\dot{\underset{\sim}{v}}$) a.c.f.'s calculated from eqn.(12) with $K_0(o)$, $K_1(o)$ and $\gamma$ as variables (see table (1)). Velocity spectra are compared

TABLE 1

Parameters for l.m.s. best fit to Molecular Dynamics Data on $C_F(t)$

| d* | $K_0(o)$ | $K_1(o)$ | $\gamma$ |
|---|---|---|---|
| 0.1 | 56.5 | 313.9 | 38.6 |
| 0.3 | 47.8 | 263.3 | 29.1 |
| 0.5 | 80.6 | 213.3 | 21.4 |
| 0.7 | 127.9 | 250.6 | 30.8 |

$K_0(o)$, $K_1(o)$, and $\gamma$ are in reduced units.

The results are at a reduced number density $p^* = 0.64$, and a reduced temperature of $T^* = 2.3$.

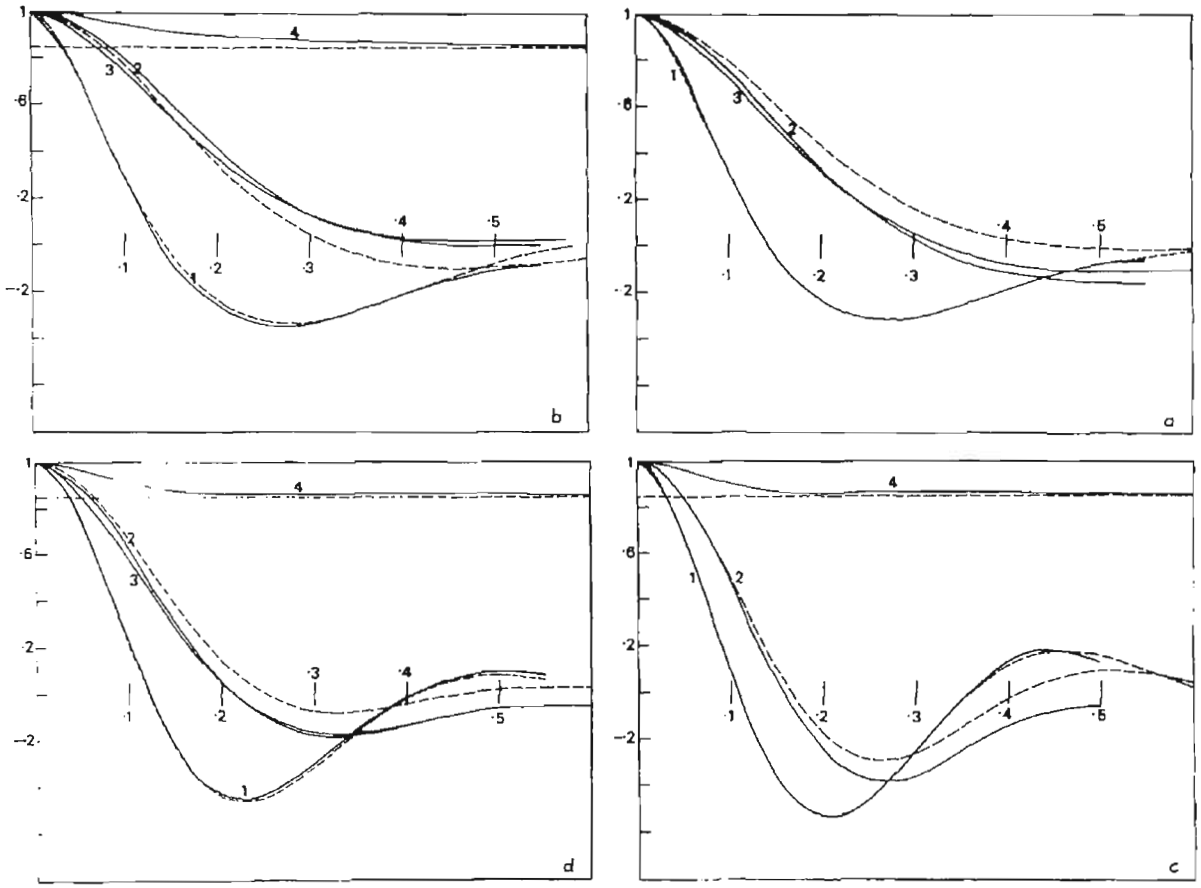


Figure (1)

(a) —— (1) Atom-atom simulation of the force a.c.f. $C_F(t)$ for a reduced interatomic separation, d*, of 0.1.

—— (2) Simulated velocity a.c.f.

—— (3) Simulated velocity-direction a.c.f.

—— (4) Simulated speed a.c.f., the horizontal line is at $8/(3\pi)$.

– – – – – (1) l.m.s. best fit of the itinerant oscillator to the simulated $C_F(t)$.

– – – – (2) $C_v(t)$ (itinerant oscillator), calculated with the $K_0(o)$, $K_1(o)$, $\gamma$ parameters estimated by fitting $C_F(t)$.

(b) d* = 0.3; (c) d* = 0.5; (d) d* = 0.7.

Ordinate: C(t); Abscissa: time steps / 200.

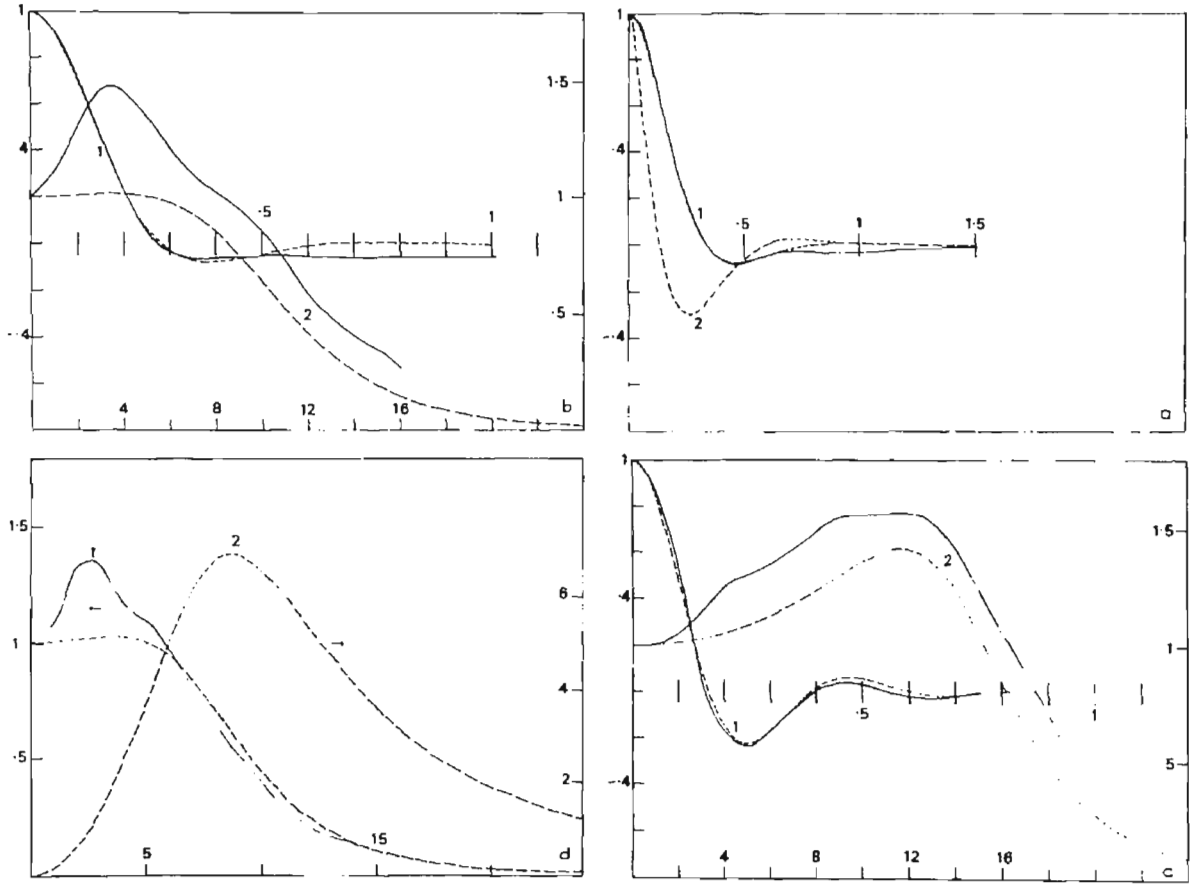


Figure (2)

(a) —— (1) Berne and Harp[10] computed velocity a.c.f. for CO.

—— (2) Computed[10], normalised velocity power spectrum.

– – – – (1) Itinerant oscillator l.m.s. best fit to the velocity a.c.f.

– – – – – (2) Corresponding normalised velocity power spectrum.

Ordinates: L.H.S.: C(t); R.H.S.: $\tilde{C}_v(\omega)/\tilde{C}_v(o)$

Abscissae: top: time/ps; bottom: freq./THz

(b) —— Rahman $C_v(t)$, simulated[8(b)] for liquid argon.

– – – (1) Itinerant oscillator, best fit.

– – – – (2) $C_F(t)$ estimated from the $C_v(t)$ best fit.

Ordinate: C(t); Abscissa: time/ps.

with those simulated by Berne and Harp[10] (on carbon monoxide), and Rahman (on argon)[8(b)] in figs. 2(a), 2(b) and 2(c). It may be shown[10,18] that at constant temperature, $K_0(o)$ is proportional to the ensemble mean square force, $\langle F^2 \rangle$, and in fig.(3), the simulated (atom-atom) $\langle F^2 \rangle$ is plotted against $K_0(o)$ obtained by fitting $C_F(t)$. The two functions are normalised at $d^* = 0.3$. The overall trend is similar, but $K_0(o)$ increases the more rapidly as $d^*$ lengthens (i.e. the more anisotropic the intermolecular potential becomes). Similarly $K_1(o)$ is related both to $\langle F^2 \rangle$ and to $\langle \dot{F}^2 \rangle$, and[19] $\gamma$ to the classical $\beta$.

Fig. 2(b) shows the 1.m.s. best fit to the velocity a.c.f. computed for liquid argon in the 864 particle simulation of Rahman[8(b)]. The extended negative tail (or low frequency peak in the velocity power spectrum) is not reproduced by 1.m.s. fitting the itinerant oscillator

---

Figure (2) continued

(c) —— Rahman simulated[8(b)] normalised velocity power spectrum.

– – – (1) Velocity power spectrum calculated from the itinerant oscillator best fit to $C_v(t)$ (fig.2(b)).

– – – – (2) Itinerant oscillator normalised force spectrum.

Ordinate: Intensity; Abscissa: frequency/THz.

(d) —— (1) Berne and Harp[10] simulated angular velocity a.c.f. for liquid CO.

– – – (1) Best fit to (1) of the itinerant librator on a plane[11(c)].

—— (2) Simulated[10] normalised angular velocity power spectrum.

– – – – (2) Itinerant oscillator normalised power spectrum calculated from fitting the a.c.f.

Ordinates: L.H.S. $C_\omega(t)$; R.H.S. $\tilde{C}_\omega(\omega)/\tilde{C}_\omega(o)$

Abscissae: Top: time/ps; bottom: $\omega$/THz.

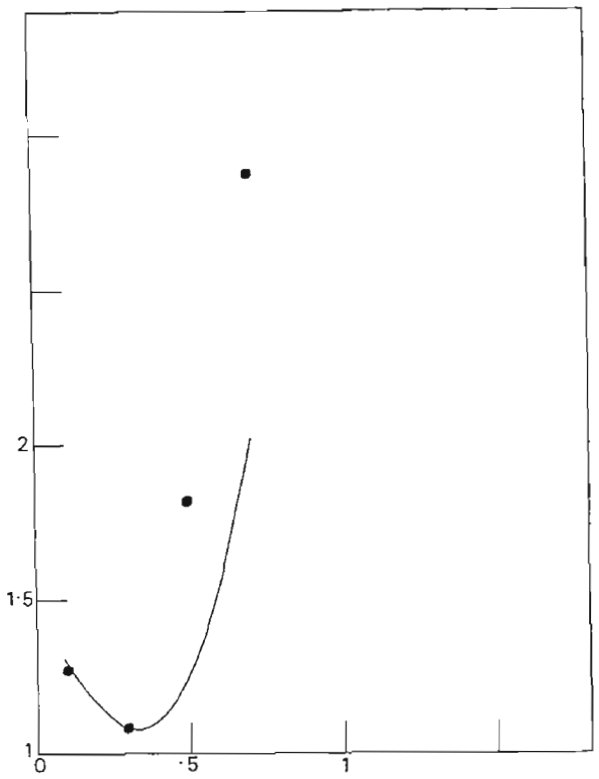


Figure (3)

Plot of $K_0(o)$ and $\langle F^{\partial} \rangle$ vs d*.

✦ $K_0(o)$; —— $\langle F^{\partial} \rangle$; normalised at d* = 0.3.

Abscissa: d*.

to the computed $C_v(t)$. Possibly, this is due to slow density fluctuations (involving the total $G(\underset{\sim}{r},t)$) set up by coupling of different modes of motion, for example, in molecules, the conversion of spin to orbital angular momentum, and coup_ling with the translational modes present[20]. The so-called 'hydrodynamic' tail is a decay from the positive side of the $C_v(t)$ axis, and thus cannot explain the intermediate negative portion. This is found again in the CO simulation (fig.2(a)) and may be discerned (figs.1(b) and figs.1(c)) in the atom-atom $C_v(t)$. In contrast (fig.2(d)), the angular velocity a.c.f. and power spectrum[10] for CO are fitted more

closely overall by the itinerant librator[12] (tractable only in two dimen_sions) developed recently by Coffey et al[19].

The parameters obtained from the l.m.s. best fit to Rahman's[8(b)] $C_v(t)$ are used in fig.4(a) to match the mean square displacement, defined by:

$$\langle \Delta r^2 \rangle = 2\int_0^t (t-\tau)\langle \underset{\sim}{v}(\tau)\cdot\underset{\sim}{v}(0)\rangle \, d\tau \qquad (20)$$

and simulated independently by Rahman[8(b)], and also (fig.4(b)), the $G_s(\underset{\sim}{r},t)$ derived experimentally by Dasannacharya and Rao[8(a)] using thermal neutrons scattered incoherently and inelastically.

It is of interest to know whether the Wiener process is, in fact, a justifiable statistical representation of random force and velocity. We adopt the method[10] of computing a.c.f.'s of moments of velocity and force to investigate this further. For example, the second moment of velocity (or kinetic energy) a.c.f.:

$$C_{2v}(t) = \langle v^2(t)v^2(0)\rangle / \langle v^4(0)\rangle$$

should be related to $C_v(t)$ by:

$$C_{2v}(t) = \frac{3}{5}\left[1 + \frac{2}{3}C_v^2(t)\right] \qquad (21)$$

were the p.d.f. of velocities a Gaussian. Similarly:

$$C_{4v}(t) = \left(225 + 600\,C_v^2(t) + 120\,C_v^4(t)\right)/945, \qquad (22)$$

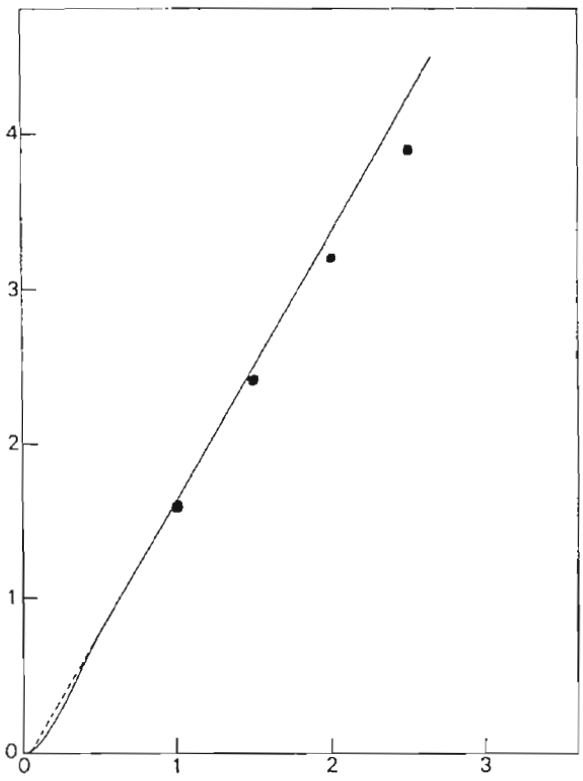


(a)

(b)

$$C_{8v}(t) = \left( 945 + 10080\, C_v^2(t) + 18144\, C_v^4(t) + 6912\, C_v^6(t) + 348\, C_v^8(t) \right) / 36465. \quad (23)$$

The functions $C_{2v}(t)$ and $C_{4v}(t)$ were calculated[16] analytically using the atom-atom $C_F(t)$ to l.m.s. optimise $K_0(o)$, $K_1(o)$ and $\gamma$. They were also simulated independently using the atom-atom algorithm, and the two sets of functions are compared in figs.5(a) to 5(c).

Discussion

Classical Brownian motion, where $C_v(t)$ decays exponentially[15], is incapable of reproducing any negative parts of the computed velocity a.c.f.'s. Further, in the classical case the mean square force is not defined, since $\exp(-\beta t)$ is not differentiable at the origin. In contrast, not only is $\langle F^2 \rangle$ well defined (through $K_0(o)$) in itinerant oscillation, but also $C_F(t)$ can be followed, by optimising $K_0(o)$, $K_1(o)$ and $\gamma$, as d*, the interatomic distance, is increased (fig.1).

---

Figure (4)

(a) Plot of mean square displacement.

— $\langle \Delta r^2(t) \rangle$ calculated from the itinerant oscillator fitting to Rahman's $C_v(t)$.

⊙ Mean square displacements computed independently by Rahman[8(b)].

Ordinate: $\langle \Delta r^2(t) \rangle$ /Å  Abscissa: time/ps.

(b) Plot of $G_s(\underset{\sim}{r},t)$ calculated for the itinerant oscillator from fitting the Rahman $C_v(t)$ function.

Ordinate: $G_s(\underset{\sim}{r},t)/\text{Å}^{-3}$; Abscissa: $\underset{\sim}{r}/\text{Å}$

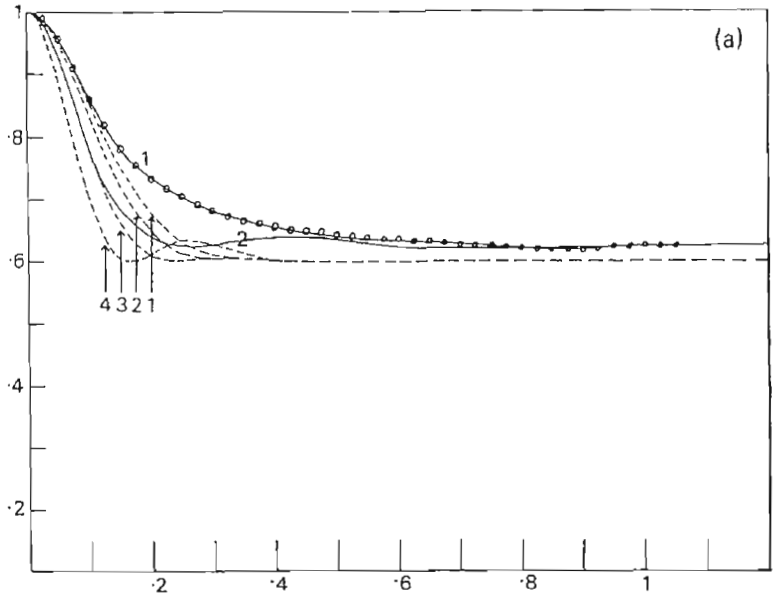


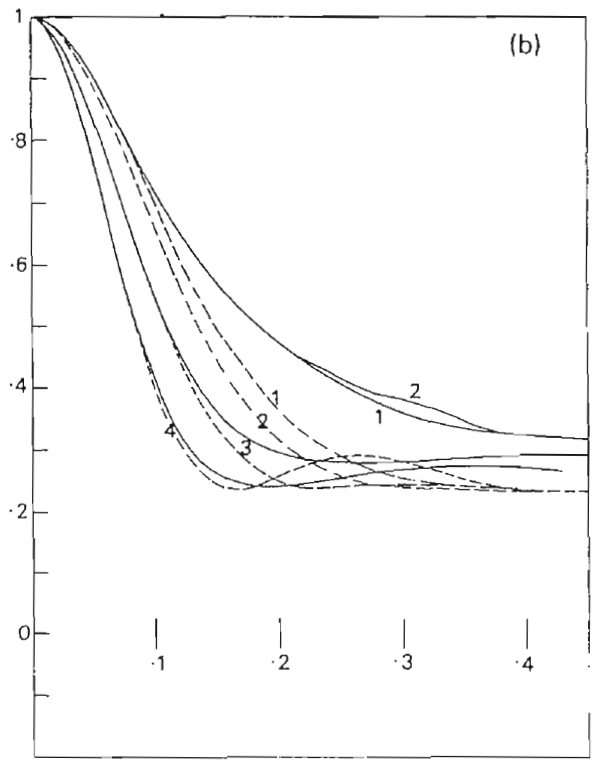


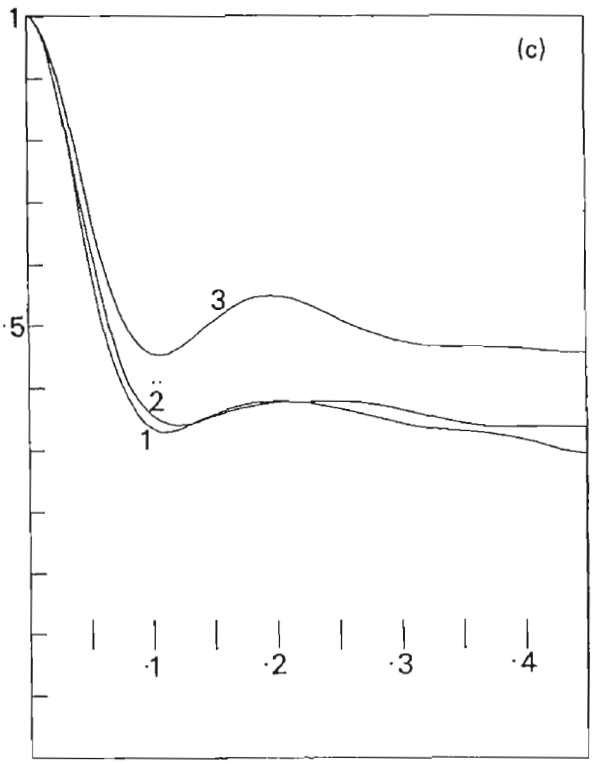


As d* increases, both $C_F(t)$ and $C_v(t)$ become more markedly oscillatory, such being the case also for the a.c.f. of the velocity direction, while in contrast the speed a.c.f. (that of $|\underset{\sim}{v}|$) consistently and quickly decays to its theoretical long time value of $8/(3\pi)$.

The similarity between $C_v(t)$ and the a.c.f. of velocity direction favours theories with a constant speed approximation, as was pointed out by Berne and Harp[10], who first suggested this type of simulation.

Knowing $C_F(t)$ analytically means that $C_v(t)$, $\langle \Delta r^2(t) \rangle$ and $G_s(r,t)$ may be calculated and compared with those independently computed or measured experimentally. In figs.1(a) - 1(d) this is done for $C_v(t)$, and it can be seen that there is a consistent small difference between the simulated $C_v(t)$, and that calculated from the optimised $C_F(t)$, although the main features are similar. At $d^* = 0.3$ and $d^* = 0.5$ there are indications of negative long time tails in the simulated $C_v(t)$.

---

Figure (5)

(a) Kinetic energy a.c.f.'s.

—— (1) $d^* = 0.1$;
—⊕— (1) $d^* = 0.3$;
—— (2) $d^* = 0.5$;

} atom-atom simulation.

– – – – (1) $d^* = 0.1$
(2) $d^* = 0.3$
(3) $d^* = 0.5$
(4) $d^* = 0.7$

} itinerant oscillator, calculated from fitting $C_F(t)$.

The horizontal line represents the Gaussian limit.

Ordinate: C(t); Abscissa: reduced time units.

(b) As for (a), $C_{4v}(t)$.

(c) $\langle F^2(t)F^2(o) \rangle / \langle F^4(o) \rangle$, atom-atom potential.

(1) $d^* = 0.1$, (2) $d^* = 0.3$, (3) $d^* = 0.5$.

Ordinate: c(t); Abscissa: time steps.

This tail is well defined for CO and argon, and causes low frequency peaks in the velocity power spectra which are not reproduced by itinerant oscillation as treated analytically in this paper. Damle et al.[3] forced an agreement with Rahman's velocity spectrum with a six parameter model of itinerant oscillation with two friction coefficients, two fluctuating forces, $\underset{\sim}{A}$ and $\underset{\sim}{B}$, and thus two memory functions corresponding to $\langle \underset{\sim}{A}(t), \underset{\sim}{A}(o) \rangle$ and $\langle \underset{\sim}{B}(t).\underset{\sim}{B}(o) \rangle$ respectively, the latter being assumed to be exponential, or Gaussian. In either case two parameters were needed for their definition. Taking this flexibility into account there is doubt as to whether the peak in the velocity power spectrum of argon may indeed be followed by a process of uncoupled linear motion, as suggested by Damle et al., or whether it is insufficient to consider $G_s(\underset{\sim}{r},t)$ as being entirely unaffected by changes in $G_d(\underset{\sim}{r},t)$, as suggested by our results. Both our treatment and that of Damle et al, neglect the cross-correlation in the <u>total</u> velocity c.f., as distinct from the auto c.f. This is tantamount to a neglect of intermolecular dynamical coherence, embodied in $G_d(\underset{\sim}{r},t)$, which is the probability of finding <u>another</u> particle at $\underset{\sim}{r}$ given there was one at the origin initially, and whose long range part in a liquid at equilibrium can be thought of as being due to spontaneous <u>macroscopic</u> density fluctuations[22].

Light and neutron scattering experiments[23] are interpretable generally in terms of the sum

$$G_s(\underset{\sim}{r},t) + G_d(\underset{\sim}{r},t) = \frac{1}{n}\langle n(\underset{\sim}{r},t)\, n(\underset{\sim}{0},0)\rangle,$$

where the time dependent particle density $n(\underset{\sim}{r},t)$ is given by:

$$n(\underset{\sim}{r},t) = \sum_i \delta(\underset{\sim}{r} - \underset{\sim}{r}_i(t)),$$

and it is never straightforward to separate $G_s(\underset{\sim}{r},t)$, usually estimated on a molecular basis, from $G_d(\underset{\sim}{r},t)$, estimated on a hydrodynamic basis. However, by use of incoherent, inelastic, neutron-scattering data from liquid argon at 84.5 K, Dasannacharya and Rao[8(a)] were able to deduce $G_s(\underset{\sim}{r},t)$ and found it to be a Gaussian within experimental error. The Rahman simulation of $C_v(t)$ is carried out at 94.4 K, but it is instructive to compare $G_s(\underset{\sim}{r},t)$ calculated from the itinerant oscillator fitting to $C_v(t)$ at 94.4 K with the $G_s(\underset{\sim}{r},t)$ estimated at 10 K lower. The results are illustrated in fig.4(b). The mean square displacement is reproduced well, but this is in any case rather insensitive to environmental effects on molecular motion compared with van Hove's functions. The overall features of the experimental $G_s(\underset{\sim}{r},t)$ are reproduced, e.g. the itinerant oscillator decays to zero at about the same $\underset{\sim}{r}$ values for given t, but the experimental $G_s(\underset{\sim}{r},t)$ is always much the larger in magnitude. The greatest difference is at t = 0.1 ps, where $G_s(\underset{\sim}{r},t)$ (exptl.) is 27 $\text{Å}^{-3}$ at $\underset{\sim}{r} = \underset{\sim}{0}$, and the itinerant oscillator about 6.5 $\text{Å}^{-3}$. Thereafter the two sets of curves become increasingly similar, so that at t = 1.0 ps, $G_s(\underset{\sim}{r},t)$ (exptl.) is 0.25 $\text{Å}^{-3}$ at $\underset{\sim}{r} = \underset{\sim}{0}$, and the itinerant oscillator 0.16 $\text{Å}^{-3}$.

Both sets of curves are Gaussian, but Rahman demonstrated that the simulated $G_s(\underset{\sim}{r},t)$ in argon displays an initial non-Gaussian behaviour lasting until 10 ps. (Unfortunately, he gives none of the $G_s(\underset{\sim}{r},t)$ functions themselves). In the atom-atom simulation fig.5(a) reveals that the kinetic energy a.c.f. $C_{2v}(t)$ is not well reproduced analytically by fitting the simulated force a.c.f., $C_F(t)$ with the itinerant oscillator. It seems that up to 200 or so time steps (1 ps or so) the Gaussian limit in $C_{2v}(t)$, 0.6, (eqn.(21)), is not reached, and this is confirmed in fig.5(b), where the simulated $C_{4v}(t)$ does not reach its equivalent limit of 0.2381 (eqn.(22)). These results show

up more clearly the limitations of the itinerant oscillator, and probably of other extended diffusion mechanisms[18] which neglect mode-mode coupling in molecular motion. In fig.5(c), the a.c.f. $\langle F^2(t)F^2(o)\rangle / \langle F^4(o)\rangle$ is displayed for $d^* = 0.1$, 0.3 and 0.5, and it is clear that no common, single-valued (or Gaussian) long-time limit is arrived at among these three potentials. Thus generally, it seems that $\underset{\sim}{v}$, $\underset{\sim}{f}$ (the projected force), and $G_s(\underset{\sim}{r},t)$ are non-Gaussian variates, as well as being non-Markovian, even in atomic fluids. If a convolution approximation[8(b)] is used to relate $G_d(\underset{\sim}{r},t)$ to $G_s(\underset{\sim}{r},t)$ via the pair distribution function g(r):

$$G_d(\underset{\sim}{r},t) = \int g(\underset{\sim}{r}')\, G_s(\underset{\sim}{r}-\underset{\sim}{r}', t')\, d\underset{\sim}{r}'$$

then $G_d(\underset{\sim}{r},t)$ is by implication also non-Gaussian. This in turn has implications for polarised light-scattering bandshapes (the Rayleigh and Brillouin peaks) since these are given essentially for point scatterers by a knowledge of the sum $G_s(\underset{\sim}{r},t) + G_d(\underset{\sim}{r},t)$, the particle density a.c.f., which can be obtained theoretically[24] by solving a generalised Langevin equation of the form:

$$\underset{\sim}{\tilde{A}}(p) = \frac{\underset{\sim}{A}(o) + \underset{\sim}{\tilde{F}}(p)}{p\,\underline{\underline{I}} + \underline{\underline{M}}} \qquad (24)$$

Here $\underset{\sim}{A}$ is a column matrix of hydrodynamic variables (usually macroscopic density, temperature, and longitudinal sound velocity parallel to the wave vector k), $\underset{\sim}{F}$ is orthogonal to $\underset{\sim}{A}$ so that $\langle \underset{\sim}{\tilde{F}}(p).\underset{\sim}{A}(o)\rangle = 0$, and $\underline{\underline{M}}$ is a matrix of hydrodynamic and thermodynamic variables[24]. Here, $\underset{\sim}{F}$ and $\underset{\sim}{A}$ are Gaussian, so that in Fourier-Laplace space, the particle density a.c.f. can be calculated as:

$$G(k,\rho) = G_s(k,\rho) + G_d(k,\rho)$$
$$= \frac{\langle n(k,\rho)\, n(k,0)\rangle}{\langle n(k,0)\, n(k,0)\rangle}$$
$$= \frac{A_0\rho^2 + B_0\rho + C_0}{D_0\rho^3 + E_0\rho^2 + F_0\rho + G_0}, \qquad (25)$$

where $A_0$, ...., $G_0$ are functions of $k$ and of phenomenological hydrodynamic and thermodynamic quantities derived macroscopically. Replacing $\rho$ by $-i\omega$ in eqn.(25) gives the Rayleigh and Brillouin lines directly. These will obviously be affected if the van Hove functions are non-Gaussian. It is interesting also to note the similarity between the hydrodynamic eqn.(25) and the molecular eqn.(7). This could well be made use of in marking out the common ground between the two species of dynamical theory: however non-Gaussian behaviour on the molecular scale will be difficult to treat analytically.

Acknowledgements

The S.R.C. is thanked for a studentship to G.J.E., the Ramsay Memorial Trust is thanked for a Fellowship to M.W.E.

Appendix

In this section we will illustrate the decay of the analytical best fit velocity p.d.f.'s and van Hove $G_s(r,t)$ functions for $d^* = 0.1$,

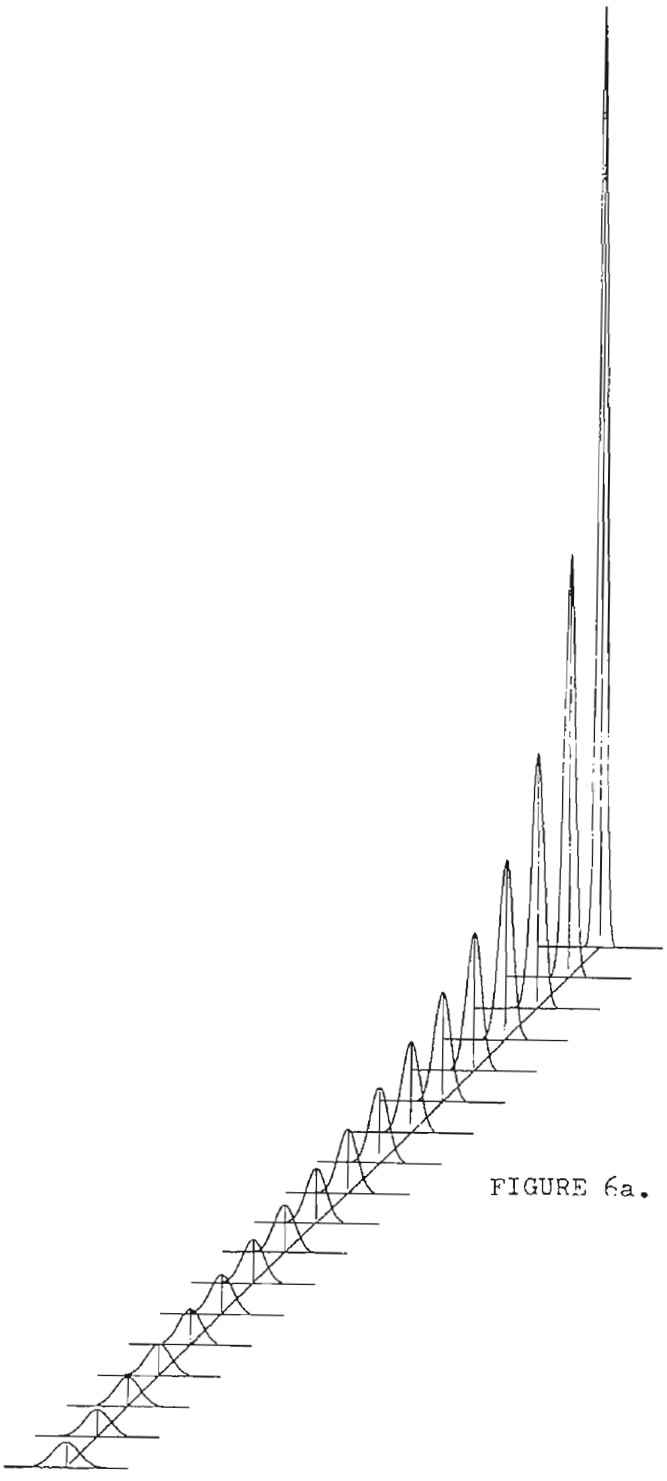

FIGURE 6a.

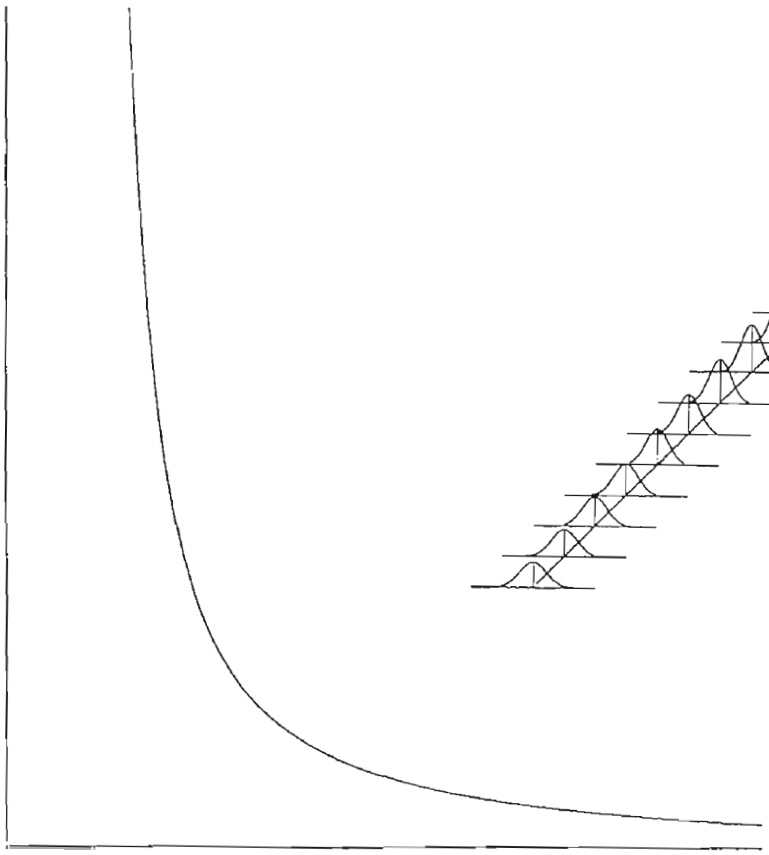

FIGURE 6b.

0.3, 0.5 and 0.7, and also for Rahman's argon simulation (fig.6). These functions contain more inherent information about the many particle dynamics than, for example, the velocity a.c.f.'s (fig.(1)) since the latter are integrals over the equivalent velocity p.d.f.'s.

References


(1) Sears, V.F., 1965, Proc. Phys. Soc., 86, 953.

(2) Frenkel, J., 1955, Kinetic Theory of Liquids, (Dover, New York).

(3) Damle, P.S., Sjölander, A., and Singwi K.S., 1968, Phys. Rev., 165, 277.

(4) Mori, H., 1965, Prog. Theor. Phys., 33, 423.

(5) Kubo, R., 1965, Statistical Mechanics of Equilibrium and Non-Equilibrium (North-Holland).

(6) Streett, W., and Tildesley, D., 1976, Proc. Roy. Soc., 348, 485.

(7) Van Hove, L., 1954, Phys. Rev., 95, 249.

(8) (a) Dasannacharya, B.A., and Rao, K.R., 1965, Phys. Rev., 137, 417;
(b) Rahman, A., 1964, Phys. Rev., 136, 405.

(9) Adelman, S.A., 1976, J. Chem. Phys., 64, 124.

(10) Berne, B.J., and Harp, G.D., 1970, Adv. Chem. Phys., 17, 63.

(11) Ford, G.W., Lewis, J.T., and McConnell, J., 1976, Proc. Roy. Ir. Acad., 76, 117.

(12) (a) Hill, N.E., 1963, Proc. Phys. Soc., 82, 723;
(b) Wyllie, G.A.P., 1971, J. Phys. C., 4, 564;
(c) Coffey, W.T., Ambrose, T., and Calderwood, J.H., 1976, J. Phys. D., 9, L115.
(d) Evans, M.W., 1977, Chem. Phys. Letters, 48, 385.

(13) Barojas, J., Levesque, D., and Quentrec, B., 1973, Phys. Rev., 7A, 1092.

(14) (a) Sack, R.A., 1957, Proc. Phys. Soc., 76, 43; 79, 402.
(b) McConnell, J., 1977, Proc. Roy. Ir. Acad., 77, 13;
(c) Wax, N., (ed.), 1954, Selected Papers on Noise and Stochastic Processes, (Dover Inc.).

(15) Uhlenbeck, G.E., and Ornstein, L.S., 1930, Phys. Rev., 36, 823.

(16) U.M.R.C.C. CDC7600, N.A.G. system, E04FAA.

(17) Cheung, P.S.Y., and Powles, J.G., 1975, Mol. Phys., 30, 921.

(18) Evans, M.W., 1977, Dielectric and Related Molecular Processes (Chem. Soc. Specialist Per. Rep., London), Vol. 3 (in press).

(19) Coffey, W.T., and Calderwood, J.H., 1977, Proc. Roy. Soc., in press.

(20) Chem. Soc. Symposium, 1976, Newer Aspects of Molecular Relaxation Processes.

(21) Rowlinson, J.S., and Evans, M.W., 1975, Chem. Soc. Ann. Rep., Sect. A, p.5.

(22) Kruus, P., 1977, Liquids and Solutions, Structure and Dynamics, (Marcel Dekker, N.Y. and Basel).

(23) Hansen, J.-P., and McDonald, I.R., 1976, Theory of Simple Liquids (Academic Press).

(24) Mountain, R.D., 1970, Chemical Rubber Co., Critical Reviews, 1, 5.